Medical Engineering and Physics 70 (2019) 72–77

Contents lists available at ScienceDirect

Medical Engineering and Physics

journal homepage: www.elsevier.com/locate/medengphy

Communication

Effect of fixed charge density on water content of IVD during bed rest: A numerical analysis

Michele Baldoni, Weiyong Gu*

Department of Mechanical and Aerospace Engineering, University of Miami, 1251 Memorial Drive, Coral Gables, FL 33146, United States

ARTICLE INFO

Article history:
Received 6 February 2019
Revised 15 May 2019
Accepted 9 June 2019

Keywords:
Multibody modeling
Intervertebral disc
Lumbar spine biomechanics
Fixed charge density

ABSTRACT

The fixed charge density (FCD) in the intervertebral disc (IVD) matrix is essential for its capacity of absorbing water, particularly during overnight bed rest. However, the FCD decreases with IVD degeneration, reducing the disc propensity to swell and the related convective transport of molecules across the IVDs. The objective of this study was to investigate the effects of the FCD on water intake in the IVD during bed rest.

A multibody musculoskeletal model was extended to include the osmotic properties of the IVDs, and used for the analysis of IVD swelling and its water content in a human subject during bed rest. The simulations were conducted with both healthy lumbar IVDs and lumbar IVDs with a reduced FCD.

It was predicted that a decrease in the FCD had a considerable impact on the IVDs swelling during bed rest. A 20% and a 45% reduction in the FCD resulted respectively in an average 25% and 55% reduction of disc water intake overnight.

This study provided an additional, quantitative information on IVD swelling in human subjects during bed rest. The computational model presented in this paper may be a useful tool for estimating disc hydration at different loading and pathological conditions.

1. Introduction

The main solid components of the extracellular matrix (ECM) of the intervertebral disc (IVD) are collagen fibers and proteoglycans (PGs) [1]. The PGs are negatively charged macromolecules, and the equivalent concentration of charged groups on PGs is known as fixed charge density (FCD). The FCD causes high osmolarity inside the tissue, which attracts water into the disc to maintain tissue hydration (i.e., swelling) [2]. This swelling behavior is essential for the IVD to support compressive loads [3].

The human spine is subjected to various loads with different postures (i.e., standing, sitting, supine) and activities during the day. Consequently, over a 24-hours period, the compressive loads on the IVDs vary greatly, causing fluid flow into and out of the IVDs. In particular, at bed rest, the compressive load on the IVDs is lower compared to that at standing, resulting in an increase in disc water content and disc height [4,5].

Disc hydration is important for the transport of molecules across the disc, as tissue hydraulic permeability and solute diffusivity depend on disc water content [6–8]. Diffusion is the main transport mechanism for small molecules (e.g., oxygen, glucose), whereas the diurnal fluid flow across the discs (associated with water content change in IVDs) could contribute considerably to the transport of large solutes (e.g., growth factors) [9]. Therefore, knowledge of disc water content is crucial to understand disc nutrition.

However, water content in IVDs changes with age, pathological and loading conditions [2,3,10–15]. Albeit quantitative results on water content increase in IVDs during bed rest have been presented in the literature [4], few studies report a quantitative analysis on the effect of the FCD on disc water absorption overnight.

Multibody musculoskeletal models are useful tools for biomechanical investigations, and have been extensively used for the analysis of the lumbar spine kinetics [16–24]. In the present study, an existing multibody model was extended to include the disc swelling behavior. The objectives of this study were to provide a quantitative tool to estimate the effect of the FCD on water content in the disc, and to investigate disc water content during bed rest.

2. Methods

In this study, the multibody musculoskeletal swelling model for human lumbar spine was developed with the AnyBody Modeling System (Version 7.1, AnyBody Technology, Aalborg, Denmark). Briefly, the model included 5 lumbar vertebrae, 198 muscle

* Corresponding author.
E-mail addresses: m.baldoni@umiami.edu (M. Baldoni), wgu@miami.edu (W. Gu).

https://doi.org/10.1016/j.medengphy.2019.06.011
1350-4533/

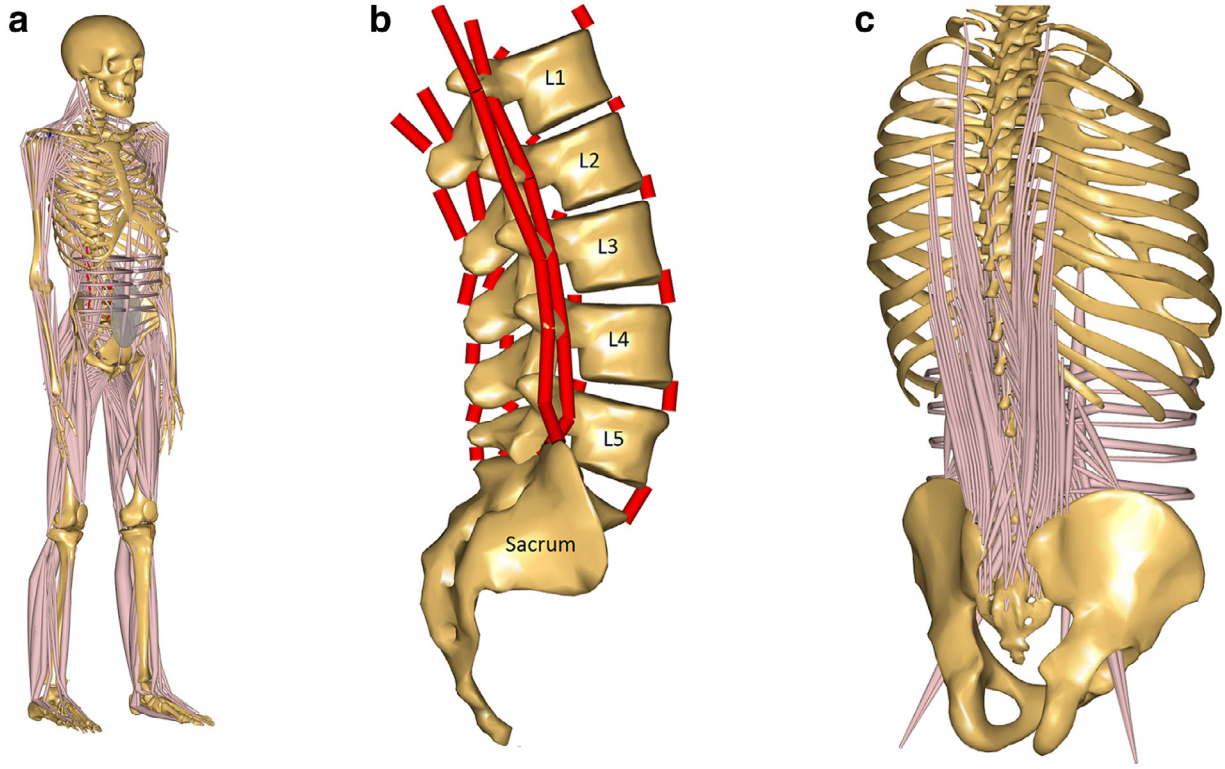

Fig. 1. (a) Full body musculoskeletal model used in this study, (b) detailed view of the lumbar vertebrae and ligaments, and (c) representation of the trunk muscles included in the model.

fascicles and 6 lumbar ligaments (supraspinous, interspinous, anterior and posterior longitudinal, intertransverse and flavum) [25] (Fig. 1).

The IVDs were represented as 6 degrees of freedom (DOFs) joints with linear elastic properties:

$$M_i = h_i \cdot \theta_i \tag{1}$$

$$F_i = k_i \cdot x_i, \tag{2}$$

where M_i is the reaction moment (Nm) and F_i the reaction force (N) generated by the IVD joint, θ_i is the rotation angle (deg) around the ith axis, x_i is the displacement (m) along the ith axis, and h_i and k_i represent the rotational and translational stiffness of the IVD, respectively. The stiffness parameters were based on data from the literature [26–28], and represent the combined stiffness of IVD and facet joints (Table 1). Note that, in Table 1, the contribution of the ligaments to the rotational stiffness was subtracted since the ligaments were modeled explicitly [29,30]. The initial height and cross-sectional area for each of lumbar discs are listed in Table 2.

Table 1
Parameters used as inputs for the simulations.

T [K]	310
c^* [mol/m^3]	150[a]
${\phi_0}^w{}_{NP}$	0.85[b]
${\phi_0}^w{}_{AF}$	0.775[b]
IVD stiffness	
Flexion [N m/deg]	0.54[c]
Extension [N m/deg]	0.78[c]
Lateral Bending [N m/deg]	0.69[c]
Axial Rotation [N m/deg]	2.52[c]
Compression/Tension [N/mm]	820[d]
Shear [N/mm]	245[e]

[a] From Zhu et al. [31].
[b] From Gu et al. [32].
[c] From Schmidt et al. [26]. 30% of the reported values were used, since ligaments are modeled explicitly [29,30].
[d] Adapted from Pollintine et al. [27].
[e] From Bisschop et al. [28].

Table 2
Lumbar discs initial height (h_0) and cross-sectional area (A_{disc}) used for the simulations.

	h_0 [mm][a]	A_{disc} [mm^2][b]
L1–L2	9	1425
L2–L3	10.4	1658
L3–L4	11.5	1714
L4–L5	11.8	1684
L5–S1	11.3	1709

[a] From Roberts et al. [33].
[b] From Pooni et al. [34].

In this study, the muscles were implemented as active force elements, and the spinal ligaments were represented as nonlinear springs (Table 3), based on the *in vitro* measurements by Chazal et al. [35].

The swelling pressure (π) of the IVD was given by [36]:

$$\pi = RT\left[\sqrt{c^{F2} + 4c^{*2}} - 2c^*\right], \tag{3}$$

where R is the universal gas constant, T the absolute temperature, c^* the concentration of salt (NaCl) in the extradiscal fluid, and c^F is the FCD. The FCD (moles per volume of fluid) is related to tissue deformation according to Lai et al. [36]:

$$c^F = c_0^F \cdot \frac{\phi_0^w}{\phi_0^w + J - 1}, \tag{4}$$

where ${c_0}^F$ is the FCD at a reference state, ${\phi_0}^w$ is the water volume fraction (i.e., water content) at the reference state, and J is the ratio of tissue volume after deformation to that at the reference

Table 3
Ligaments stiffness (K) implemented in the model, based on *in vitro* measurements by Chazal et al. [35].

Ligament	*K* [N/mm]	Strain [%]	K [N/mm]	Strain [%]	*K* [N/mm]	Strain [%]
ALL	36.2	0–11	115.9	11–41	43	41–51
PLL	52.7	0–11	127	11–28	37.1	28–37
IS	13	0–14	38.5	14–36	10.3	36–48
SS	13	0–14	38.5	14–36	10.3	36–48
FL*	23.4	0–8	54.5	8–20	12.5	20–25
IT*	12.5	0–9	61.4	9–15	25	15–17

ALL=anterior longitudinal ligament; PLL=posterior longitudinal ligament; IS=interspinous; SS=supraspinous; FL=flavum; IT=intertransverse.
* Per side.

state. An increase in the IVDs cross-sectional area during bed rest has been reported in the literature [37], and in this study, we assumed that when the IVD imbibes water (swelling), the percentage changes in its dimension are approximately the same in all three principal directions. Therefore, the volume ratio (J) of the disc may be estimated by:

$$J = \left(\frac{h}{h_0}\right)^3, \tag{5}$$

where h is the disc height and h_0 is the disc height at the reference state. The water volume fraction of the IVD (ϕ^w) can be calculated as follows (after Lai et al. [36]):

$$\phi^w = \frac{\phi_0^w + J - 1}{J}. \tag{6}$$

Considering the normal direction of the IVD (perpendicular to the upper surface of the disc), at equilibrium (i.e., no fluid loss or gain) we can write:

$$F_{ext} = F_S + F_E, \tag{7}$$

where F_{ext} is the normal component of the compressive force acting on the IVD due to body weight, muscle forces, and ligament forces, F_s is the force (in the normal direction) generated by the swelling pressure, and F_E is the elastic force (due to disc deformation) in the normal direction (Eq. (2)). Since lumbar vertebrae facets have been reported to be loaded in disc compression and spine extension [38–40], the facet contact forces were neglected in this study.

The magnitude of the swelling pressure depends on the FCD (Eq. (3)), which is constant in the nucleus pulposus (NP) and almost linearly decreases towards the outer annulus fibrosus (AF) [12]. The corresponding swelling pressure follows the same trend (Fig. 2), and therefore an average value of FCD in the AF may be used to estimate the mean value of π in the AF. Based on Urban and Maroudas' results for a healthy IVD [12], the average FCD in the AF corresponds to the 80% of the FCD in the NP.

Therefore, the IVD swelling force, F_s, can be expressed as:

$$F_S = \pi_{NP} \cdot A_{NP} + \pi_{AF} \cdot A_{AF}, \tag{8}$$

where π_{NP} and π_{AF} are the swelling pressures in the NP and AF, respectively, and A_{NP} and A_{AF} are the cross-sectional areas of the NP and the AF, respectively. Considering that the NP occupies approximately 40% of the IVD cross-sectional area [34,41,42], combining Eqs. (3) and (8) we have:

$$F_S = A_{disc} RT \left[0.4\left(\sqrt{c_{NP}^{F2} + 4c^{*2}} - 2c^*\right) + 0.6\left(\sqrt{c_{AF}^{F2} + 4c^{*2}} - 2c^*\right)\right], \tag{9}$$

where A_{disc} is the IVD cross-sectional area, $c^F{}_{NP}$ is the mean FCD in the NP, and $c^F{}_{AF}$ is the mean FCD in the AF (which is assumed to be 80% of $c^F{}_{NP}$).

Table 4
Values of FCD in the NP at the reference state ($c_0{}^F{}_{NP}$) calculated from the FCD per tissue dry weight and the hydration reported in Urban and McMullin [2]. The values in the table represent the average of the values, at each lumbar level, reported in Urban and McMullin [2] for discs up to 37 years of age.

Level	L1–L2	L2–L3	L3–L4	L4–L5	L5–S1
$c_0{}^F{}_{NP}$ [mol/m^3]	261	242	239	215	217

The average water volume fraction of the IVD can be estimated by:

$$\phi^w = 0.4 \cdot \phi_{NP}^w + 0.6 \cdot \phi_{AF}^w, \tag{10}$$

where $\phi_{NP}{}^w$ and $\phi_{AF}{}^w$ are the water volume fraction in the NP and in the AF, respectively.

The swelling force F_s was calculated by Eqs. (4) and (9) using $c_0{}^F{}_{NP}$ values calculated from literature measurements (Table 4) [2]. The F_{ext} in the standing posture (i.e., the reference state) was predicted at all lumbar levels (with a model simulation) by introducing offset forces required to prevent relative motion of adjacent vertebrae [43]. The correspondent elastic force F_E in the standing posture, due to the compression of the disc solid matrix, was calculated by Eq. (7).

The bed rest was simulated by a subject lying on a supporting surface (Fig. 3). The initial curvature of the spine was assumed to be the same as the curvature in standing. The method for treating the contact between body and supporting surface was the same as that described by Rasmussen et al. [44]. Briefly, contact elements were defined between a series of points along the body and the supporting surface (Fig. 3). The contact elements were modeled as artificial muscles capable of exerting compressive and frictional forces, and these contact forces were calculated as part of the muscle optimization process (see below). The friction coefficient between the body and the support was assumed to be 0.5 [45].

The muscle and joint reaction forces in the system were calculated by an inverse dynamics process [46] in AnyBody. A third-order polynomial criterion was used in this study for muscle optimization [47,48]. The spinal ligaments were assumed to be in their undeformed state in the standing posture (i.e., the reference state) [49]. The kinematics of the 6-DOFs lumbar joints was predicted based on the equilibrium of forces and moments acting on the lumbar spine. Thus, the present musculoskeletal model allowed to predict the changes in IVDs height (and therefore J, Eqs. (5) and (7)) and in the lumbar curvature during bed rest, at equilibrium.

Based on the *in vitro* measurements of the decrease of the FCD with age reported by Urban and McMullin [2] for a 25, 44 and 68 years old spines, three cases were simulated:

(1) Normal lumbar discs (with FCD values listed in Table 4)
(2) 20% reduction in the FCD in all lumbar discs
(3) 45% reduction in the FCD in all lumbar discs.

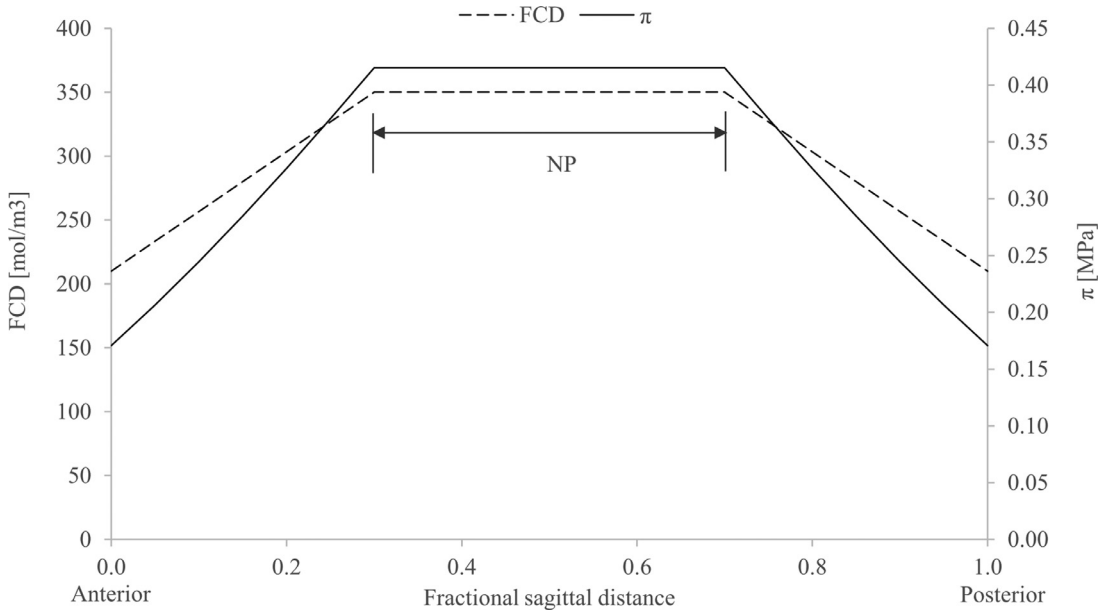

Fig. 2. Fixed charge density (FCD) distribution in the sagittal direction for a 27 year-old IVD, adapted from [12], and corresponding swelling pressure (π) distribution calculated from Eq. (3). For a linear decrease of the FCD from the NP to the outer AF, a quasi-linear decrease in the swelling pressure is calculated.

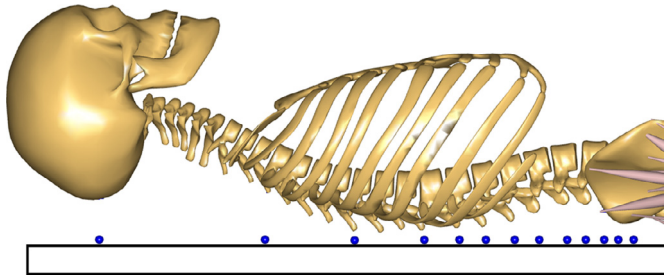

Fig. 3. Representation of the resting support and contact points for the spine used in the bed rest simulation. The contact points are distributed along the spine in correspondence of the cranium and the vertebrae: T2, T6, T9, T10, T11, T12, L1, L2, L3, L4, L5, Sacrum. Arms and muscles are not shown for clear visualization.

3. Results

A human subject of 174 cm and 72 kg was simulated. The material properties and parameters were reported in Tables 1 and 2. During standing, the compressive force (F_{ext}) was predicted to range between 387 N and 431 N among the lumbar IVDs. The calculated values of F_E ranged between 57 N and 181 N among the 5 lumbar discs (Table 5).

During bed rest, F_{ext} was predicted to range between 61 N and 136 N among the lumbar IVDs (Table 6). The predicted water content in normal lumbar IVDs (Eq. (10)) ranged from 82.2% to 82.4% during bed rest (increased from an overall value of 80.5% at standing), corresponding to an averaged 9.9% increase in IVD volume compared to standing. The increase in water content (i.e., the difference in water volume fraction) ranged from 1.7% to 1.9%. For the case of a 20% decrease in FCD, the increase in IVD water content was predicted to range between 1.2% and 1.4% (average 7.3% IVD volume increase), while it ranged between 0.7% and 1% (average 4.2% IVD volume increase) in case of a 45% reduction of the FCD (Fig. 4).

Table 5
Predicted compressive forces (F_{ext}) at each lumbar level during standing, and correspondent elastic forces calculated from Eq. (7).

Level	F_{ext} [N]	F_E [N]
L1–L2	406	98
L2–L3	388	57
L3–L4	387	83
L4–L5	409	164
L5–S1	431	181

Table 6
Predicted compressive forces (F_{ext}) at each lumbar level during bed rest.

Level	F_{ext} [N]
L1–L2	61
L2–L3	73
L3–L4	78
L4–L5	95
L5–S1	136

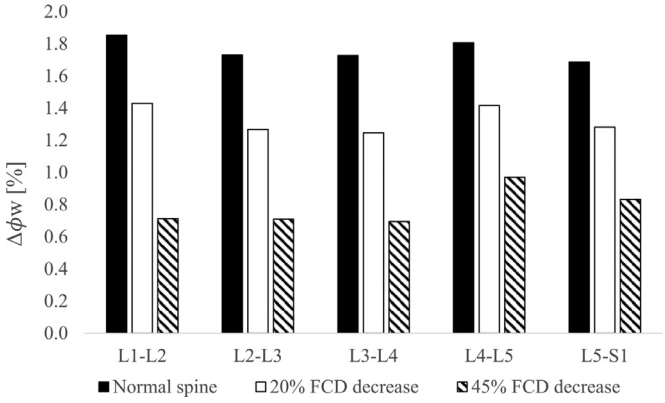

Fig. 4. Predicted water content (i.e., water volume fraction) increase during bed rest (at equilibrium) for a normal spine, and for the cases of 20% and 45% decreases in the FCD.

4. Discussion

In this study, a multibody musculoskeletal model was extended to include the IVD swelling behavior, and employed to investigate

the effect of FCD on the water content in IVDs during bed rest. With decreasing FCD, the IVDs swelled less during overnight bed rest, resulting in smaller amount of fluid intake in IVDs. For example, if FCDs in lumbar discs are reduced by 45%, the averaged fluid intake is reduced by ~55% (from 1.7–1.8% to 0.7–1.0%, see Fig. 4), compared to the intake in normal discs. The IVD's water absorption during bed rest is considered an important mechanism for the convective transport of large solutes. The present study shows that when the FCD content decreases, the capacity of the IVD to imbibe fluid overnight declines, possibly impairing the convective transport of molecules into the disc [9]. Moreover, this investigation confirms that bed rest plays an important role in disc nutrition [4].

The calculated average volume increase (9.8%) in normal lumbar discs is comparable with the in vivo measurement of disc volume increase (3.6–16.9%, average: 10.6%) in five normal subjects aged 21–32 years, after at least 8-h overnight bed rest on a hospital bed [4]. This indicates that the presented model is capable of predicting disc swelling with reasonable accuracy, even though some simplifications and assumptions have been made in the analysis.

In this study the IVD was modeled as a linear elastic structure, instead of a more realistic nonlinear material. Effort shall be made in the future to improve the accuracy of the model predictions.

In summary, the present study introduced a new multibody approach for the investigation of the role of the FCD on the IVD's swelling properties. The predicted volume change in normal lumbar disc at bed rest is consistent with the results reported in the literature. The decrease of the FCD (associated with PG content) in the IVDs was predicted to have a substantial impact on the discs capacity of absorbing fluid during overnight bed rest, possibly affecting the supply of nutrients to the disc. The computational approach presented in this paper may be a useful tool in predictive analyses of disc swelling behavior and its related spine biomechanics.

Acknowledgement

Research reported in this publication was supported by the National Institute of Arthritis and Musculoskeletal and Skin Diseases of the National Institutes of Health under Award Number AR066240. The content is solely the responsibility of the authors and does not necessarily represent the official views of the National Institutes of Health.

Conflict of interest statement

No financial support or benefits have been received from any commercial source related directly or indirectly to the scientific work reported in this manuscript.

Ethical approval

Not required.

References

[1] Redaelli A, Montevecchi F. Biomeccanica analisi multiscala di tessuti biologici. Patron Editore; 2007.
[2] Urban JP, McMullin JF. Swelling pressure of the lumbar intervertebral discs: influence of age, spinal level, composition, and degeneration. Spine 1988;13:179–87.
[3] Urban JP, Roberts S. Degeneration of the intervertebral disc. Arthritis Res Ther 2003;5:120–30.
[4] Malko JA, Hutton WC, Fajman WA. An in vivo MRI study of the changes in volume (and fluid content) of the lumbar intervertebral disc after overnight bed rest and during an 8-hour walking protocol. J Spinal Disord Tech 2002;15:157–63.
[5] Belavy DL, Armbrecht G, Richardson CA, Felsenberg D, Hides JA. Muscle atrophy and changes in spinal morphology is the lumbar spine vulnerable after prolonged bed-rest? Spine 2011;36:137–45.
[6] Lai WM, Mow VC. Drag-induced compression of articular cartilage during a permeation experiment. Biorheology 1980;17:111–23.
[7] Gu W, Yao H, Huang C, Cheung H. New insight into deformation-dependent hydraulic permeability of gels and cartilage, and dynamic behavior of agarose gels in confined compression. J Biomech 2003;36:593–8.
[8] Gu WY, Yao H. Effects of hydration and fixed charge density on fluid transport in charged hydrated soft tissues. Ann Biomed Eng 2003;31:1162–70.
[9] Urban J, Holm S, Maroudas A, Nachemson A. Nutrition of the intervertebral disc: effect of fluid flow on solute transport. Clin Orthop Relat Res 1982:296–302.
[10] Lyons G, Eisenstein SM, Sweet MB. Biochemical changes in intervertebral disc degeneration. Biochim Biophys Acta 1981;673:443–53.
[11] Urban JP, McMullin JF. Swelling pressure of the inervertebral disc: influence of proteoglycan and collagen contents. Biorheology 1985;22:145–57.
[12] Urban JPG, Maroudas A. The measurement of fixed charged density in the intervertebral disc. Biochim Biophys Acta (BBA) – Gen Subj 1979;586:166–78.
[13] Wang Y-XJ, Griffith JF, Leung JC, Yuan J. Age related reduction of T1rho and T2 magnetic resonance relaxation times of lumbar intervertebral disc. Quant Imaging Med Surg 2014;4:259.
[14] Jarman JP, Arpinar VE, Baruah D, Klein AP, Maiman DJ, Tugan Muftuler L. Intervertebral disc height loss demonstrates the threshold of major pathological changes during degeneration. Eur Spine J 2015;24:1944–50.
[15] Vergroesen P-PA, van der Veen AJ, Emanuel KS, van Dieën JH, Smit TH. The poro-elastic behaviour of the intervertebral disc: a new perspective on diurnal fluid flow. J Biomech 2016;49:857–63.
[16] McGill SM, Norman RW. Effects of an anatomically detailed erector spinae model on L4 L5 disc compression and shear. J Biomech 1987;20:591–600.
[17] Bogduk N, Macintosh JE, Pearcy MJ. A universal model of the lumbar back muscles in the upright position. Spine 1992;17:897–913.
[18] Stokes IA, Gardner-Morse M. Lumbar spine maximum efforts and muscle recruitment patterns predicted by a model with multijoint muscles and joints with stiffness. J Biomech 1995;28:177–86.
[19] Plamondon A, Gagnon M, Desjardins P. Validation of two 3-D segment models to calculate the net reaction forces and moments at the L5S1 joint in lifting. Clin Biomech 1996;11:101–10.
[20] Keller TS, Nathan M. Height change caused by creep in intervertebral discs: a sagittal plane model. J Spinal Disord 1999;12:313–24.
[21] Huynh KT, Gibson I, Lu WF, Jagdish BN. Simulating dynamics of thoracolumbar spine derived from LifeMOD under haptic forces. World Acad Sci Eng Technol 2010;4:236–43.
[22] Delp SL, Anderson FC, Arnold AS, Loan P, Habib A, John C, et al. OpenSim: open-source software to create and analyze dynamic simulations of movement. IEEE Trans Biomed Eng 2007;54:1940–50.
[23] Arshad R, Zander T, Bashkuev M, Schmidt H. Influence of spinal disc translational stiffness on the lumbar spinal loads, ligament forces and trunk muscle forces during upper body inclination. Med Eng Phys 2017;46:54–62.
[24] Gagnon D, Arjmand N, Plamondon A, Shirazi-Adl A, Larivière C. An improved multi-joint EMG-assisted optimization approach to estimate joint and muscle forces in a musculoskeletal model of the lumbar spine. J Biomech 2011;44:1521–9.
[25] de Zee M, Hansen L, Wong C, Rasmussen J, Simonsen EB. A generic detailed rigid-body lumbar spine model. J Biomech 2007;40:1219–27.
[26] Schmidt TA, An HS, Lim TH, Nowicki BH, Haughton VM. The stiffness of lumbar spinal motion segments with a high-intensity zone in the anulus fibrosus. Spine 1998;23:2167–73.
[27] Pollintine P, van Tunen MS, Luo J, Brown MD, Dolan P, Adams MA. Time-dependent compressive deformation of the ageing spine: relevance to spinal stenosis. Spine 2010;35:386–94.
[28] Bisschop A, Mullender MG, Kingma I, Jiya TU, van der Veen AJ, Roos JC, et al. The impact of bone mineral density and disc degeneration on shear strength and stiffness of the lumbar spine following laminectomy. Eur Spine J 2012;21:530–6.
[29] Heuer F, Schmidt H, Klezl Z, Claes L, Wilke HJ. Stepwise reduction of functional spinal structures increase range of motion and change lordosis angle. J Biomech 2007;40:271–80.
[30] Ignasiak D, Dendorfer S, Ferguson SJ. Thoracolumbar spine model with articulated ribcage for the prediction of dynamic spinal loading. J Biomech 2016;49:959–66.
[31] Zhu Q, Jackson AR, Gu WY. Cell viability in intervertebral disc under various nutritional and dynamic loading conditions: 3d finite element analysis. J Biomech 2012;45:2769–77.
[32] Gu W, Zhu Q, Gao X, Brown MD. Simulation of the progression of intervertebral disc degeneration due to decreased nutritional supply. Spine 2014;39:E1411–17.
[33] Roberts N, Gratin C, Whitehouse GH. MRI analysis of lumbar intervertebral disc height in young and older populations. J Magn Reson Imaging 1997;7:880–6.
[34] Pooni JS, Hukins DW, Harris PF, Hilton RC, Davies KE. Comparison of the structure of human intervertebral discs in the cervical, thoracic and lumbar regions of the spine. Surg Radiol Anat 1986;8:175–82.
[35] Chazal J, Tanguy A, Bourges M, Gaurel G, Escande G, Guillot M, et al. Biomechanical properties of spinal ligaments and a histological study of the supraspinal ligament in traction. J Biomech 1985;18:167–76.

[36] Lai WM, Hou JS, Mow VC. A triphasic theory for the swelling and deformation behaviors of articular cartilage. J Biomech Eng 1991;113:245–58.
[37] LeBlanc AD, Evans HJ, Schneider VS, Wendt RE 3rd, Hedrick TD. Changes in intervertebral disc cross-sectional area with bed rest and space flight. Spine (Phila Pa 1976) 1994;19:812–17.
[38] Yang KH, King A. Mechanism of facet load transmission as a hypothesis for low-back pain. Spine 1984;9:557–65.
[39] Adams M, Hutton W. The effect of posture on the role of the apophysial joints in resisting intervertebral compressive forces. Bone Jt J 1980;62:358–62.
[40] Dunlop RB, Adams MA, Hutton WC. Disc space narrowing and the lumbar facet joints. J Bone Joint Surg Br 1984;66:706–10.
[41] De Palma AF, Rothman RH. The intervertebral disc. W. R. Saunders Co.; 1970.
[42] Bogduk N. Clinical anatomy of the lumbar spine and sacrum. Edinburgh: Churchill Livingstone; 1997.
[43] Dao TT. Enhanced musculoskeletal modeling for prediction of intervertebral disc stress within annulus fibrosus and nucleus pulposus regions during flexion movement. J Med Biol Eng 2016;36:583–93.
[44] Rasmussen J, Tørholm S, De Zee M. Computational analysis of the influence of seat pan inclination and friction on muscle activity and spinal joint forces. Int J Ind Ergon 2009;39:52–7.
[45] Ishihara S, Ishihara K, Nagamachi M. Finite element estimation of pressure distribution inside the trunk on a mattress. Int J Autom Smart Technol 2015;5:217–23.
[46] Otten E. Inverse and forward dynamics: models of multi–body systems. Philos Trans R Soc Lond B: Biol Sci 2003;358:1493–500.
[47] Damsgaard M, Rasmussen J, Christensen ST, Surma E, de Zee M. Analysis of musculoskeletal systems in the anybody modeling system. Simul Model Pract Theory 2006;14:1100–11.
[48] Rasmussen J, Damsgaard M, Voigt M. Muscle recruitment by the min/max criterion - a comparative numerical study. J Biomech 2001;34:409–15.
[49] Putzer M, Ehrlich I, Rasmussen J, Gebbeken N, Dendorfer S. Sensitivity of lumbar spine loading to anatomical parameters. J Biomech 2016;49:953–8.